Research Square

Preprints are preliminary reports that have not undergone peer review.
They should not be considered conclusive, used to inform clinical practice,
or referenced by the media as validated information.

A robust framework for evaluating marine heatwave risk in surface and seafloor waters.

Stephanie Woolley

stephanie.woolley@utas.edu.au

University of Tasmania https://orcid.org/0009-0009-0865-6059

Moninya Roughan

UNSW Australia https://orcid.org/0000-0003-3825-7533

Robert Mason

University of New South Wales

Nicholas Perkins

University of Tasmania

Tim Ingleton

Department of Climate Change Engery Environment and Water

Skipton Woolley

CSIRO

Joel Williams

University of Tasmania https://orcid.org/0000-0002-4173-3855

Article

Keywords:

Posted Date: October 28th, 2026

DOI: https://doi.org/10.21203/rs.3.rs-10915846/v1

License: This work is licensed under a Creative Commons Attribution 4.0 International License.
Read Full License

Additional Declarations: There is **NO** Competing Interest.

A robust framework for evaluating marine heatwave risk in surface and seafloor waters.

Author Information

Authors: Stephanie H. Woolley[1*], Moninya Roughan[2], Robert A. B. Mason[2], Nicholas Perkins[1], Tim Ingleton[3], Skipton N.C Woolley[4], Joel Williams[1].

* stephanie.woolley@utas.edu.au

[1] Institute for Marine and Antarctic Science, University of Tasmania, Hobart, Tasmania, Australia,7000

[2] School of Biological Earth and Environmental Sciences, University of New South Wales, Sydney, NSW, Australia, 2052

[3] Department of Climate Change, Energy, the Environment and Water (DCCEEW), Waters, Wetlands and Coastal Science, New South Wales, Sydney, NSW, Australia

[4] Environment Research Unit, Commonwealth Scientific and Industrial Research Organisation, Battery Point, Tasmania, Australia, 7000

Contributions

S.H.W developed the framework, performed the analyses, validation and manuscript writing. M.R contributed to the oceanographic interpretation, validation approach, supervision and manuscript review and editing. R.M contributed to the framework methodology, interpretation of analyses, and manuscript review and editing. T.I and N.P contributed to supervision, interpretation of results, and manuscript review and editing. S.N.C.W contributed to manuscript reviewing and editing. J.W contributed the framework methodology, interpretation of results, supervision, and manuscript review and editing. J.W., M.R, and T.I acquired funding supporting the research. All authors discussed the results and approved the final manuscript.

Target Journal: Nature Climate change

Abstract

Marine heatwaves (MHWs) are intensifying globally, yet risk assessments often rely on sea surface temperature data and individual metrics that may not represent sub-surface or seafloor exposure especially across depth gradients. This is increasingly limiting for assessing impacts on benthic ecosystems, where thermal extremes may be decoupled from sea surface conditions. Here we present a framework applicable to surface and seafloor temperature data, that integrates metrics of frequency, duration and intensity alongside the seasonal cycle and long-term temperature trends to produce a MHW hazard index. Demonstrating the utility in three regions across the southeast Australian continental shelf, this framework highlights MHW hazards are spatially heterogenous across regions and depth gradients. These differences show that surface-based hazards fail to represent seafloor dynamics, challenging our use of surface metrics in ecosystem risk assessments. This framework provides a standardised approach for representing MHW hazard that can be readily applied in other regions globally.

Introduction

It is well documented that increasing marine heatwaves (MHWs), defined as extended periods of anomalous warm water above the 90th percentile for over five days, are having profound ecological and socioeconomic impacts[1–3]. Global models project a 16 to 41 fold increase in MHW probability, and longer, more intense events into the future[4]. As MHWs are known to be state-altering events, causing mass mortality and shifts in species distributions[2,5–7], understanding the risk of these events is developing into a key research and management area. Risk has been broadly defined as the potential for MHWs to cause adverse ecological or socioeconomic impacts, where risk is often described as a combination of three

inputs: hazards, exposure, and vulnerability[8]. Hazards are often represented by a single MHW metric, exposure as the likelihood of a community or species being exposed to the events[8]. Vulnerability as the consequence or impact of the events to those species or communities based on species or community specific responses such as thermal thresholds or recovery capacity[8–11]. However, often this means that the hazard component of MHW risk assessments is defined by a single surface-based oceanographic metric which often misrepresents seafloor dynamics[9,12–14]. This approach may therefore be prone to oversimplification and misrepresentation of the risk MHWs pose to benthic communities across different depths and within different oceanographic systems.

MHW risk has commonly been assessed through event-based classification, short-term risk forecasting, or species hazard frameworks[12,15,16]. Event-based approaches such as the definitions described by Hobday et al[15,17] provide a standardised method to classify the severity of individual MHW events based on their intensity, thereby increasing awareness of the risks they pose. This classification has supported the development of forecasting tools that categorise the risk of future events. These tools provide a likelihood of an event occurring in given days, weeks or months based on differences in the current sea surface temperature (SST) compared to the long-term average or from future predicted SST conditions[16,18–21]. While these approaches are valuable for identifying risk and supporting short-term response plans, they primarily assess risk as a product of discrete event occurrence and surface conditions. This provides opportunities for short term mitigation strategies but limits their application as they lack insight into how MHWs (and therefore risk) varies below the surface, particularly at the seafloor.

The usefulness of these risk frameworks and our current understanding of MHW events and metrics is limited by our ability to quantify these events below the surface. Until recently

most large-scale assessments of MHWs have been focused on the surface, largely due to long spatially and temporally continuous (satellite-derived) temperature datasets[3,22]. In contrast, subsurface temperature observations remain sparse and unevenly distributed, with long term moorings providing the most temporally continuous record available to resolve how temperatures and thus MHWs vary through the water column[22,23]. Mooring observations have shown that many deeper ecologically important reefs are now known to experience more intense MHWs than their surface counterparts[13,24,25], where MHWs are shaped by vertical stratification, wind anomalies and boundary currents[14,26,27]. These processes often drive vertical differences within the water column which result in variations in the timing, intensity and persistence of MHWs between surface and the seafloor[14]. The different MHW types have been classified into six categories distinguished by the depth, and vertical extents, where notably some events occur without a surface signature[28]. Two of these classifications of MHWs; full depth and benthic MHWs occur directly at the seafloor and as such are likely to have the largest impact on benthic communities with the remaining types limited to potential indirect impacts[28]. The contrasting event structure highlights the complexity of sub surface MHWs and their potential risk to benthic ecosystems.

Benthic ecosystems support a diverse range of fish and invertebrate assemblages, yet for deeper communities, particularly those below thermal mixed layers, their exposure to MHW is often poorly resolved[29]. This limited understanding is particularly critical in subsurface environments where local oceanographic dynamics are decoupled from surface temperature conditions[30]. Deeper benthic ecosystems, particularly communities across the continental shelf (30-200m) support a wide range of competing socioeconomic activities and are exposed to a variety of other compounding anthropogenic threats like overfishing and sedimentation from coastal land use[24,31]. . For these communities understanding variation in the timing,

intensity and duration of MHWs at the seafloor is particularly important as management of MHW events is often only achievable through the mitigation of other stressors[32,33]. Furthermore, these deeper benthic ecosystems are poorly represented in marine management and current areas of protection are often incidental rather than targeted[34]. This leads to a lack of monitoring and little long-term ecological data which increases the difficulty of quantifying MHW impacts and the potential risk across different depths[35,36].

Ecologically-integrated MHW risk assessments and hazard frameworks often include species specific data alongside temperature and MHW metrics such as life history stages and mortality, providing critical insights for industries dependent on those species[9,12]. Research using risk frameworks are often for specific purposes, with studies for specific taxon or industry stakeholders, and are therefore constructed with defined temperature thresholds or with outputs that look at temperature exceedance for specific species[9,12]. While these provide robust risk frameworks for specific communities they often limit their broader application due to dependence on either singular surface-based metrics or application to shallow water species [9,21]. Furthermore, these frameworks are inherently only applicable to well-studied ecological communities as they are reliant on a baseline understanding of oceanographic conditions and thermal thresholds, which may potentially lead to a lack of representation and applicability of risk assessments for vulnerable or rare species that could face greater consequences from MHW events. Therefore, there is a need for more generalised risk frameworks that are represented by a combination of oceanographic variables likely to be more widely transferable across different regions and taxonomic groups.

MHW risk frameworks remain limited by the use of one metric (derived from SST data) to represent whole MHW hazards. Furthermore, the singular use of SST data restricts our ability to assess variance in risk towards benthic communities across deep seafloor gradients. To

address this, here we develop and validate a transferable risk framework for spatial assessments of MHWs and illustrate its use both at the surface and seafloor. This is applied across three oceanographically distinct regions along the temperate east coast of Australia (spanning 29°S and 38°S). The East Australian Current (EAC), its separation zone, and southern extension is a good test region as it is a known hotspot of global warming with complex dynamic and competing space use including a network of MPAs. By integrating multiple MHW metrics with seasonal thermal structure and long-term warming trends, this framework aims to provide both an assessment of seafloor hazard structure and a tool for future risk assessment and management use, applicable to surface and seafloor regions globally.

Results

MHW Risk framework

The MHW risk framework provides a spatially explicit index of the relative hazard across surface and seafloor temperature regimes across a continental shelf (Figure 1). The framework integrates five components of thermal exposure: the frequency, duration, and intensity of events as well as the local thermal structure of seasonality and long-term warming trends (Figure S1:3). This accounts for event-driven hazards relative to local conditions. These components produce a relative spatial hazard index (SHI) for oceanographic-based risk assessments for use as the hazard component in broader risk assessments.

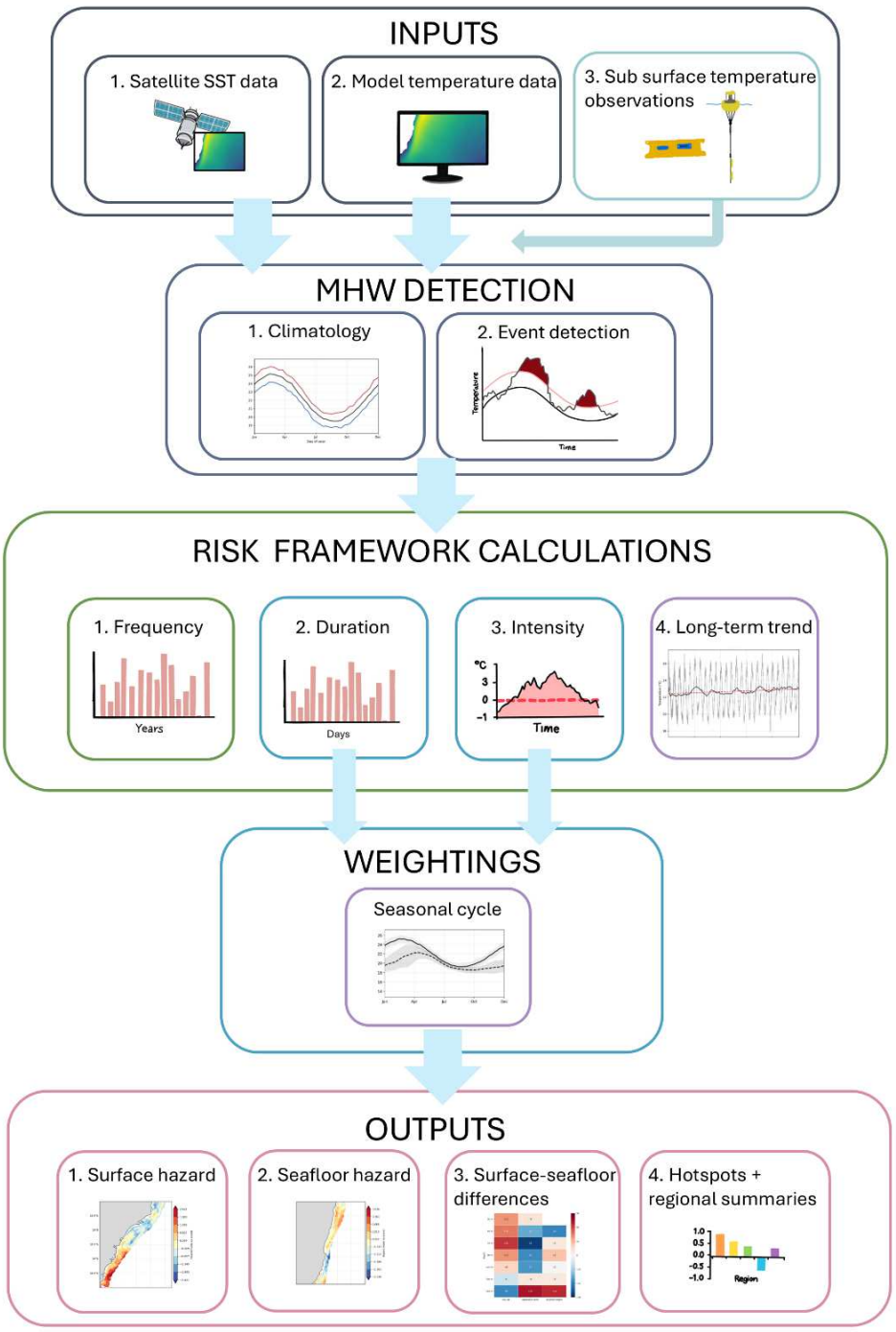


Figure 1: Conceptual workflow of the MHW risk framework. Top row shows the integration of three sources of temperature data, where satellite SST data and model temperature directly feed into the framework and in situ sub surface observations contribute to the validation and development of modelled temperature data. The second row shows the identification of MHW events following the definitions by Hobday et al 2016. The third row indicates the three core components of the risk framework of frequency, duration and intensity and the secondary variable of the long-term temperature trend. The fourth row shows the weighting of the seasonal cycle where it is applied to the duration and intensity metrics from row three. The Bottom row shows the four key outputs of the spatial hazard index for the surface and seafloor, and summaries of risk across different regions.

MHW hazard patterns

Across all regions of the continental shelf of the temperate east, the hazard index exhibited a clear difference between the surface and the seafloor, with no shared pattern or spatial structure and a disparity greatest in regions of the outer continental shelf (Figure 2). Across the EAC jet the index at the surface was heterogeneous across different latitudes with a marked area of high MHW hazard south of 31°S. In contrast, the seafloor had a latitudinal pattern with a higher index in the region of 29°S to 30.8S°. In the separation zone, the MHW hazard index at the surface had a distinct latitudinal pattern with a transition from low to high hazard at 33.6°S, whereas at the seafloor there was strong cross shelf gradient with a higher hazard index at the shelf edge and a lower inshore index. Across the EAC southern extension surface patterns revealed more moderate index values with a marked area of high hazard along the shelf edge particularly at 35°S and a marked area of low index around 37.5°S. At the seafloor there were differing spatial patterns with areas of high hazard at around 36°S and 37.3°S with lower relative hazard between and towards 38°S.

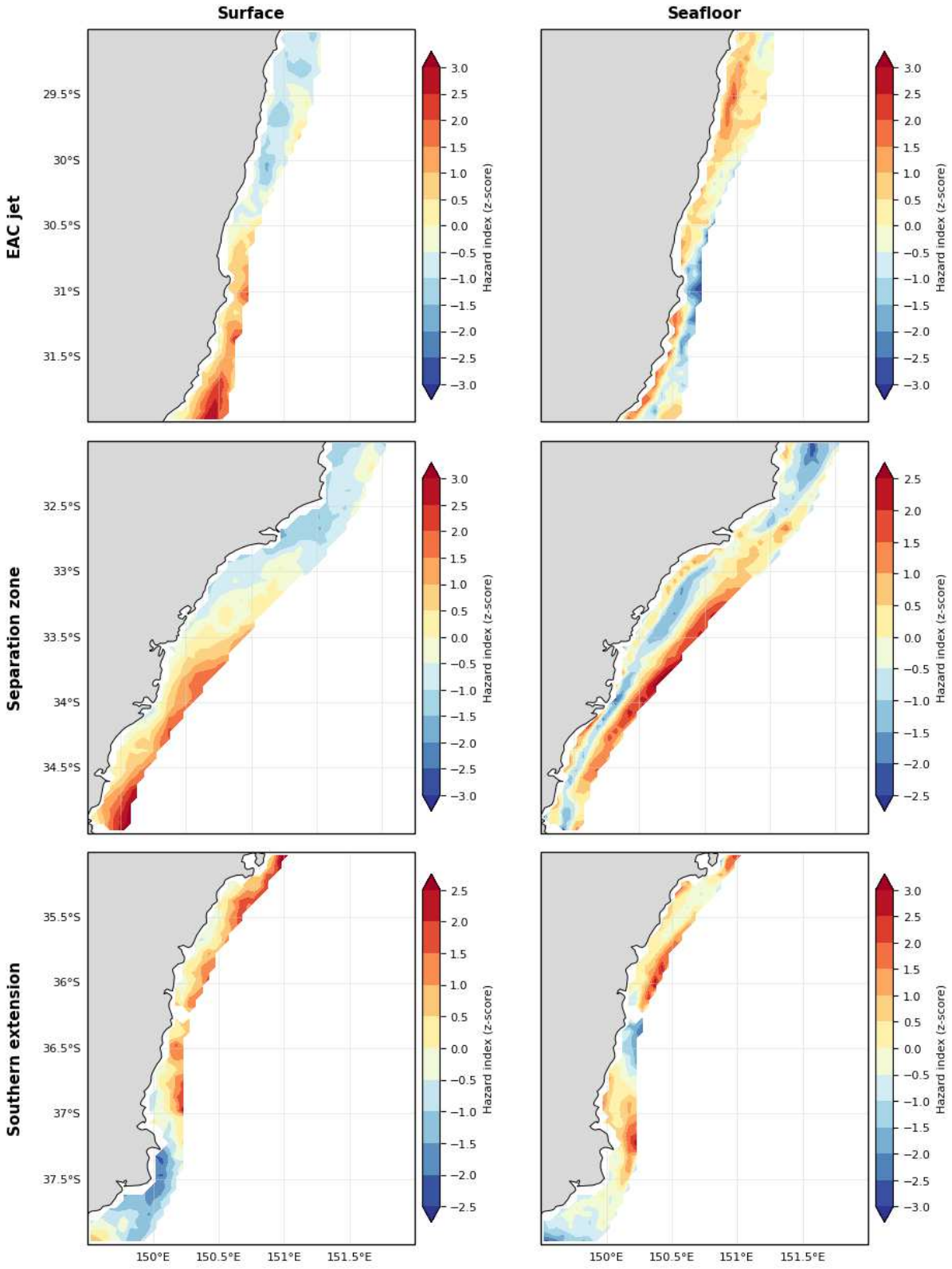


Figure 2: Spatial hazard index maps of the three selected study regions, developed from the MHW risk framework, where each region and depth has a relative risk score created where individual grid cells have a corresponding hazard score relative to the regional mean. Areas outside of the shelf (between the 30-200 m isobaths) are masked. Positive values indicate areas of higher-than-average risk while negative values indicate areas of lower-than-average risk.

Surface and seafloor divergence across the continental shelf

Overall, there were significant differences in the relative position of surface and seafloor hazards and this varied both across the three different regions and the corresponding seafloor depth (Figure 3). In the EAC jet region, had the largest divergence between surface and seafloor hazard index values. Seafloor values were highest between 30 and 70m along the continental shelf, the SHI then decreased to 190m at the shelf edge. Surface SHI was inverse with lowest hazard between 30 and 70m which then increased with depth. The surface SHI was highest at the isobathic depth of 150m whereas seafloor SHI was highest at 70m, whereas only at 90m isobathic depth did both the surface and seafloor report similar negative hazard values (Figure 3, top panel).

The separation zone had some divergence between surface and seafloor hazard index values but saw a similar pattern of increasing SHI across the shelf except for the seafloor at 70m where there was a positive SHI (Figure 3). The highest risk was at the shelf edge at 190m for both the seafloor and the surface, but shallower shelf regions saw greater variation in hazard (Figure 3, middle panel). In the southern extension index values were relatively closer with less divergence between surface and seafloor values across most seafloor depths (Figure 3, lower panel). The greatest divergence occurred at 50m and then between 50-190m both surface and seafloor values were close to their respective means (Figure 3, lower panel).

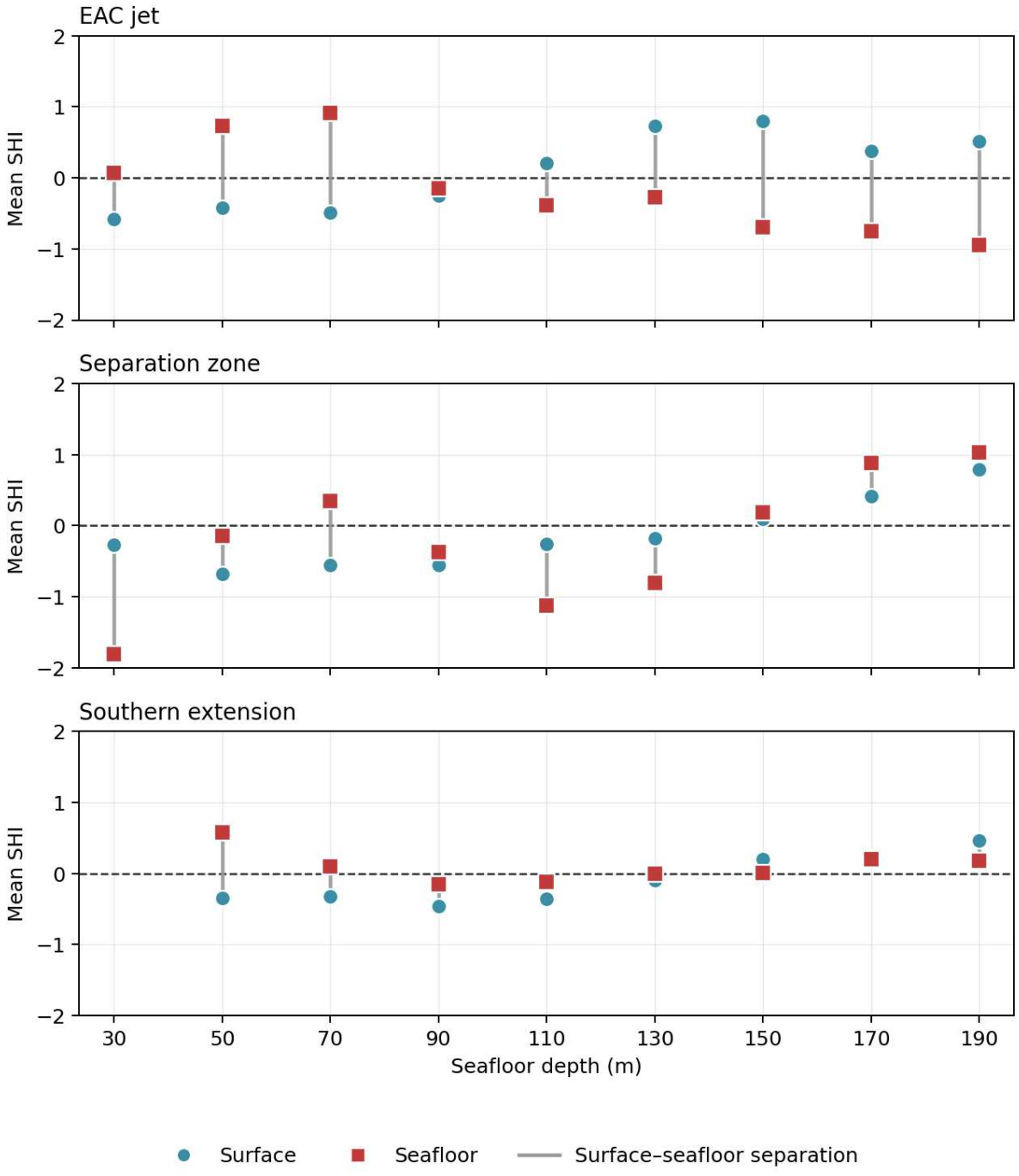


Figure 3: Mean relative spatial hazard across the seafloor for the three (oceanographically distinct) regions. Where surface values correspond to the surface grid cells directly above at that specific seafloor depth. Red and blue points show mean hazard index value with grey horizontal lines displaying the separation between surface and seafloor values. As the hazard index was standardised separately for each region and depth, differences should be interpreted as the divergence in the relative hazard rankings. Therefore, points below the mean represent a lower hazard within its own regional index rather than the difference in thermal exposure between the surface and seafloor indexes.

Discussion

Marine heatwaves (MHWs) are increasingly recognised as vertically complex events, where temperature conditions can vary differently at the surface compared to below the surface and at the seafloor[25,27,28]. Yet currently our understanding of the risk MHWs pose to benthic communities is often from sea surface temperature (SST) data or based on very limited subsurface data[6,37]. This is a potential limitation as research has found MHW events can extend well beyond the surface mixed layer, be decoupled from surface conditions, or intensify near the seafloor (with no surface expression), thus producing dramatically different seafloor signatures and impacts[25,26,38]. Our findings here reinforce the conclusion that surface MHW metrics can misrepresent seafloor metrics, even across relatively small spatial regions resulting in significantly different risk signatures. Differing surface and seafloor hazard patterns suggest that surface-based assessments may incorrectly estimate or spatially misplace the hazard to benthic communities. As such risk assessments reliant solely on SST data likely provide a misleading representation of MHW exposure for benthic communities.

In regions where surface and seafloor temperature (and hence hazard) patterns were more closely aligned, it likely reflects regional ocean dynamics such as areas with weak stratification and stronger vertical coherence[14,39], rather than evidence that SST data is able to represent benthic MHW hazard more broadly. Furthermore, our results highlight current limitations in MHW and climate risk assessments, where although SST data remains central to large-scale MHW detection and monitoring it provides an incomplete basis for assessing risk to sub surface and benthic environments. This is especially the case across stratified systems and shelf-edge environments, where surface temperature anomalies may be weakly coupled to seafloor thermal conditions[14]. As a result, global and regional assessments that rely solely on SST data may overlook important depth variation in MHW exposure which

when coupled with limited ecological data for deeper benthic communities[1,35] increases the chance of misrepresentation in current ecosystem risk assessments.

Beyond highlighting the limitations of using SST data to represent seafloor hazards, our research shows that different MHW metrics contribute regionally to the overall MHW hazard. Across the selected study regions spatial variation was structured by differing metrics particularly at the seafloor. Incorporating a multitude of MHW metrics allows for the capturing of different hazard drivers where needed, or applying greater emphasis on particular ecologically meaningful MHW metrics. The need for a multi-metric approach is further supported by current research which shows different physical processes generate and maintain MHWs differently across depth[25,38,40,41]. Surface MHWs are often associated with air-sea heat fluxes and reduced wind-driven mixing[42,43], whereas seafloor events can further be driven by subsurface processes such as horizontal advection of warm water, relaxation or variation in cross shelf processes (such as upwelling or downwelling) and eddy activity[27,38]. This variability likely contributes to the spatial variation in the framework, furthermore, accounting for seasonal timing and variability within the framework was important as research shows that MHWs have differing seasonal impacts with summer MHW events considered potentially more ecologically severe. Therefore, the inclusion of multiple MHW metrics and regional temperature variability strengthens the application and reliability of this framework across different oceanographic regions and captures the complexity of thermal extremes that single metric frameworks and assessments may miss.

Currently risk assessments for both climate and extreme events within the ocean are often limited by their region or species of study[9,12,44], this results in no universal method of estimating risk to benthic communities. The most common and widely used risk assessment framework outlined by the IPCC integrates components of hazard, exposure, and

vulnerability[8], however, studies often define these individual components differently with inputs ranging from single MHW metrics and only surface data to depth resolved models with hazard defined as temperature above a specific species driven threshold[9,10]. This often limits the wider application of these assessments. Our results from the east coast of Australia illustrate a framework that can be applied to other regions globally, due to the integration of long-term trends and seasonality defined by the regional oceanographic conditions. This further aligns with climate risk studies that often assess hazards as departures from baseline conditions while accounting for interannual variability[45]. Therefore, this framework not only integrates important MHW metrics and regional variability that was previously missing from MHW risk assessments but can help define hazards within wider extreme event risk assessments that combine this hazard with ecological data.

MHW and oceanographic risk assessments were developed based on the need to identify ecological communities most at risk of exposure and adverse impacts from extreme events. However, until recently, these have been focused on shallow benthic communities due to the availability of long-term ecological data and the feasibility of using SST data. Deeper reef environments such as mesophotic ecosystems are key ecological communities that support unique fish and invertebrate assemblages and are socioeconomically important, particularly for commercial and recreational fisheries[46,47]. Understanding MHW impacts and risk to these communities is therefore becoming increasingly urgent. Currently, research shows mesophotic reefs are at risk of prolonged exposure to extreme events, redistribution of key species, and bleaching within temperate and tropical communities[24,48,49]. However broader spatial or community level assessments are often hindered by a lack of long-term empirical data, as technology has only recently enabled the quantification of mesophotic environments[29]. Due to this, current management and monitoring plans for these ecosystems

are often limited, and the use of standard risk assessment frameworks that rely on community-specific vulnerability indices are not yet feasible. The risk framework developed and demonstrated here addresses this by providing a greater spatial understanding of the distribution of extreme events for mesophotic reef environments but also an applicable screening tool to identify and direct ecological monitoring to regions where the risk from thermal extremes is likely to be the greatest.

Understanding MHW impacts is an important aspect to the management of deeper ecosystems, for both conservation and fisheries[50–52]. By resolving the current spatial structure of MHW hazard this framework can be used to identify where current protected areas overlap with high hazard locations, areas of low exposure and potential refuge. However, continued research is needed to link apparent hazards with ecological observations and habitat mapping, this can be done by incorporating vulnerability and exposure indices alongside this framework into larger management plans. Furthermore, sustaining the availability of subsurface temperature records is critical for improving and validating model-based spatial assessments and enhancing our understanding of extreme events below the surface and at the seafloor. Strengthening and building long-term oceanographic and ecological data will provide more accurate, management ready risk assessments of MHW risk for deeper reef ecosystems and thereby enable sustainable ecosystem management in a rapidly changing climate.

Methods

Study region

To examine the framework across a variety of oceanographic settings, it was applied to three dynamically different oceanographic regions across the southeast Australian continental shelf between 29°S and 38°S, 150°E and 160°E and 30-200m depth (Figure 4). The three regions

were defined as the East Australian Current (EAC) jet, north of -32°, and the separation zone south of 32°S, and the southern extension south of 35°S. The exact latitude that defines the separation zone varies seasonally, where it is commonly centred at 32.5°S with the range from 31°S to 33°S[53,54], here we use south of 32°S for simplicity. The continental shelf circulation is dominated the EAC and its associated eddy field, which drives strong latitudinal gradients in circulation, temperature variability and MHW metrics. The EAC jet is several tens of kilometres wide extending from the surface to ~300 m deep, carrying warmer, more saline water from the subtropics into the Tasman sea[54,55]. Thermal extremes in this region are influenced by the strength, position and variability of the EAC jet, with surface MHWs often driven by air-sea heat fluxes and subsurface MHWs are driven by eddy-modulated EAC advection[40,56]. The separation zone is a transition region from a coherent jet dominated region to an eddy-dominated flow where the EAC diverges from the coast, and circulation is driven by mesoscale eddies responsible for most cross-shelf heat exchange, driving warm subsurface intrusions and localised upwelling. These processes vary interannually and therefore contribute to strong spatial variability in ocean heat content and can generate deep, persistent MHWs across the shelf and upper slope. The EAC Southern extension is dominated by anticyclonic eddies and is a known warming hotspot that is warming 2-4 times faster than global average[57]. MHWs in this region are often driven by these mesoscale eddies[58]. These three regions were selected to evaluate the framework's ability to capture spatial variation and patterns in regions with differing oceanographic conditions. Furthermore, it provides an ideal case study area due to the combined availability of high-resolution oceanographic models, satellite observations and long-term in situ mooring records for validation.

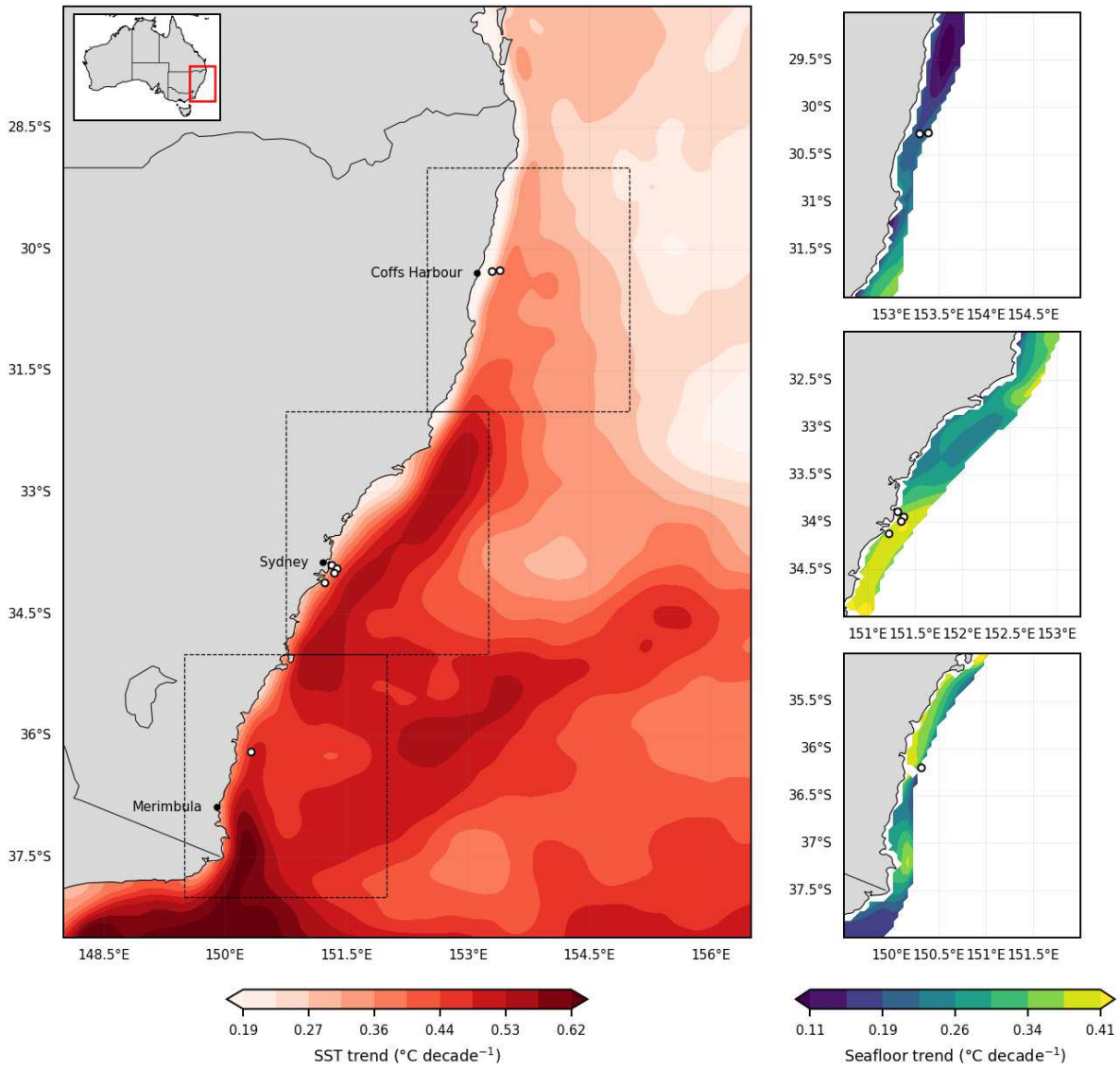


Figure 4: Surface and seafloor temperature trends across the 26-year period (1994-2019). The left panel shows the SST trends of the region with three bounding boxes representing the three oceanographic regions explored in the risk framework. White points represent the corresponding mooring locations used for validation. The right three panels are the seafloor trend for the two selected regions subset to the on-shelf regions chosen between 30 to 200m.

Data sources

A combination of satellite, in situ and modelled temperature data was used within the framework as they provide spatio-temporal coverage over the full depth of the water column from the surface to the seafloor. For this study, satellite-derived temperature data was obtained from the NOAA Coral Reef Watch CoralTemp product, which provides daily, gap-filled sea surface temperature (SST) observations derived from multiple satellite sensors at approximately 5km spatial resolution[59].

Subsurface temperature was obtained from a 26-year (1994-2019) free-running simulation of the SEA-COFS (Southeast Australia-Coastal Ocean Forecasting System) which is a hydrodynamic model configuration of the Regional Ocean Modelling System (ROMS) for the East Australian Current System[60]. It provides high resolution (5-12km) three-dimensional oceanographic fields, including temperature, salinity and currents, tailored for the southeast Australian shelf and slope. It is a dynamically consistent representation of ocean variability and as such is suitable for MHW characterisation. Although we cannot expect a free-running simulation to reproduce the exact timing, duration and intensity of marine temperature extremes, this is not a concern in this study as it is focused on the statistical properties of marine temperature extremes. Model-derived potential temperature was converted to in situ temperature using the TEOS-10 formulation and package where in situ temperature is derived from potential temperature, practical salinity and pressure[61].

In situ subsurface temperature observations were obtained from seven long-term oceanographic moorings deployed along the east coast of Australia, with two mooring off Coffs harbour at approx. 30.3°S (CH070, CH100), four off Sydney at approx. 34.0°S (SYD100, SYD140, ORS065, and PH100), and one off Merimbula at approx. 36.2°S (BMP120), these were downloaded from the AODN (Australia Ocean Data Network) maintained by IMOS (Integrated Marine Observing Systems).

In situ temperature validation

Model derived MHW statistics were evaluated against in situ observations from the oceanographic moorings (Figure 4)[62]. Moorings with a minimum of 10-years of temperature data were used to determine the broad MHW trends and metrics at the closest observational depth to the seafloor. Although a 30-year baseline is typically recommended for MHW

characterisation, shorter time series (>10 years) have been shown to provide a sound estimate of MHW metrics[63]. Climatology and MHW detection were constructed using a 30-day moving window with the model climatology calculated across the same temporal window corresponding to each individual mooring dataset. MHW events were identified following Hobday et al[15] for both the model and the observations.

Model data were averaged across a fixed spatial area around each mooring, where modelled temperature data were extracted from grid cells within a 25km² circular area, with an approximate radius of 2.8km. Modelled temperature values were extracted at the vertical layer closest to the corresponding mooring depth and averaged across the retained model cells. This provided a spatially aggregated estimate of local temperature conditions at the depth of each mooring. Modelled MHW frequency and mean duration were generally comparable and showed good agreement with the in-situ temperature observations (Figure 5). A further comparison of MHW severity categories across the four event types of moderate, strong, severe and extreme[17] also had good agreement with the mooring observations with a slight overestimation of moderate events by the model (Figure 5). Therefore, we concluded that the model captured the general patterns of MHW events through the water column and supported its use within the seafloor MHW risk framework.

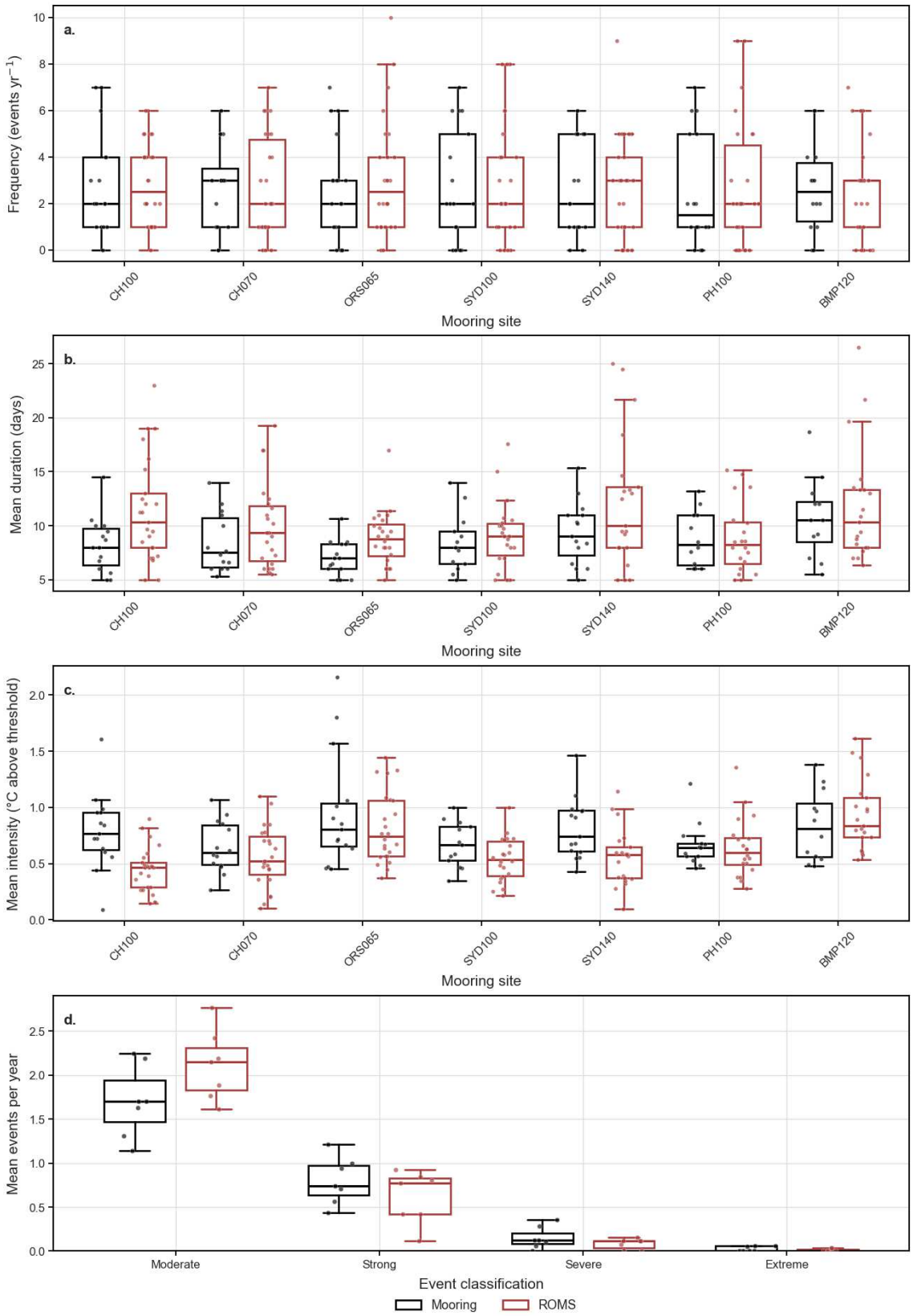


Figure 5: Comparison of seven mooring sites along the East Australian coast to the corresponding model depth and metrics. Each point represents the model or mooring annual statistics. Panel a., b., c. are the three main MHW metrics of frequency, mean duration and mean intensity. Panel d. represents the distribution of the four types of MHW events where each point is the mean number of events per year for each mooring model combination, where black boxes represent the moorings and red the model.

Climatology and marine heatwave detection

MHWs across the total timeseries were identified following the Hobday et al (2016) classification where daily mean climatology and 90th percentile threshold was calculated with a 30-day smoothing window across the 26-year run period of the SEA-COFS model. Events were identified as periods of five days or longer where the temperature is above the 90th percentile threshold with a minimum of three days between events[15]. The intensity, duration and frequency of MHWs were quantified across the 26-year period.

Risk framework development

MHW risk was evaluated using an additive standardised spatial risk framework, which integrates multiple MHW metrics and thermal exposure applicable for both surface and subsurface spatial temperature data. This approach was used to preserve the contribution of each MHW metric which removes the interaction assumption of multiplicative indices where high hazards would only occur where all inputs are simultaneously high. Such an assumption would potentially negate the influence of different types of exposure such as in regions where MHWs are highly persistent but relatively short events. This would disproportionately amplify extreme values and increase sensitivity to uneven metric distributions, where the use of an additive framework preserves the contribution of each MHW metric. Within this framework, relative hazard was defined as the combined influence of recurrent, persistent and intense thermal extremes, modified by the seasonal thermal dynamics and long-term warming trends at each grid cell. The framework was constructed from three event-derived MHW metrics of frequency, duration and intensity and two secondary climate modulators of seasonality and long-term warming. The quantitative output from the framework, referred to as the spatial hazard index (SHI) was therefore defined as:

$$SHI = z\left(\left[z\left(\frac{F}{T}\right) + z(\bar{D}) + z(\bar{I})\right] \times W\right) \quad (1)$$

Where F/T represents the mean frequency of events across the 26 years, $(\bar{D})$ is the weighted mean duration of events and $(\bar{I})$ is the weighted mean intensity, where the weights are set to 1 here for equal contribution but can be altered to increase weighting of certain metrics. This is useful in scenarios where certain metrics may cause higher ecological stress to a focal study species and thus would be more important within the framework. The overline represents the application of the seasonal weighting to the duration and intensity metrics. W represents the climate warming term and z denotes z-score standardisation. Prior to calculation, all input metrics of mean frequency, weighted mean duration and intensity were evaluated for skewness or zero inflation within each region and across surface and seafloor data. No skewness or influential outliers were identified and therefore no pre-transformation was applied. The metrics were independently z-standardised to allow variables measured in different units to be combined. The final SHI were standardised relative to the regional distribution of risk values, where the SHI values therefore represent the relative MHW risk as deviations from the regional mean.

Seasonality was included in the framework to account for the timing of MHW events relative to the local annual temperature cycle. Spatially MHWs in warmer periods are expected to be more detrimental than those that occur in cooler periods, however, across different seafloor depths, seasonal cycles and strengths vary (Figure 6). This was assessed across three latitudinal bands, off the coast of at approx. 30.0°S, 33.8°S, and 36.9°S (off the coast of Coffs Harbour, Sydney and Merimbula: Figure 4). The risk framework accounts for this by assessing the seasonal cycle at each grid cell and redistributing risk based on the warmest and coolest periods experienced.

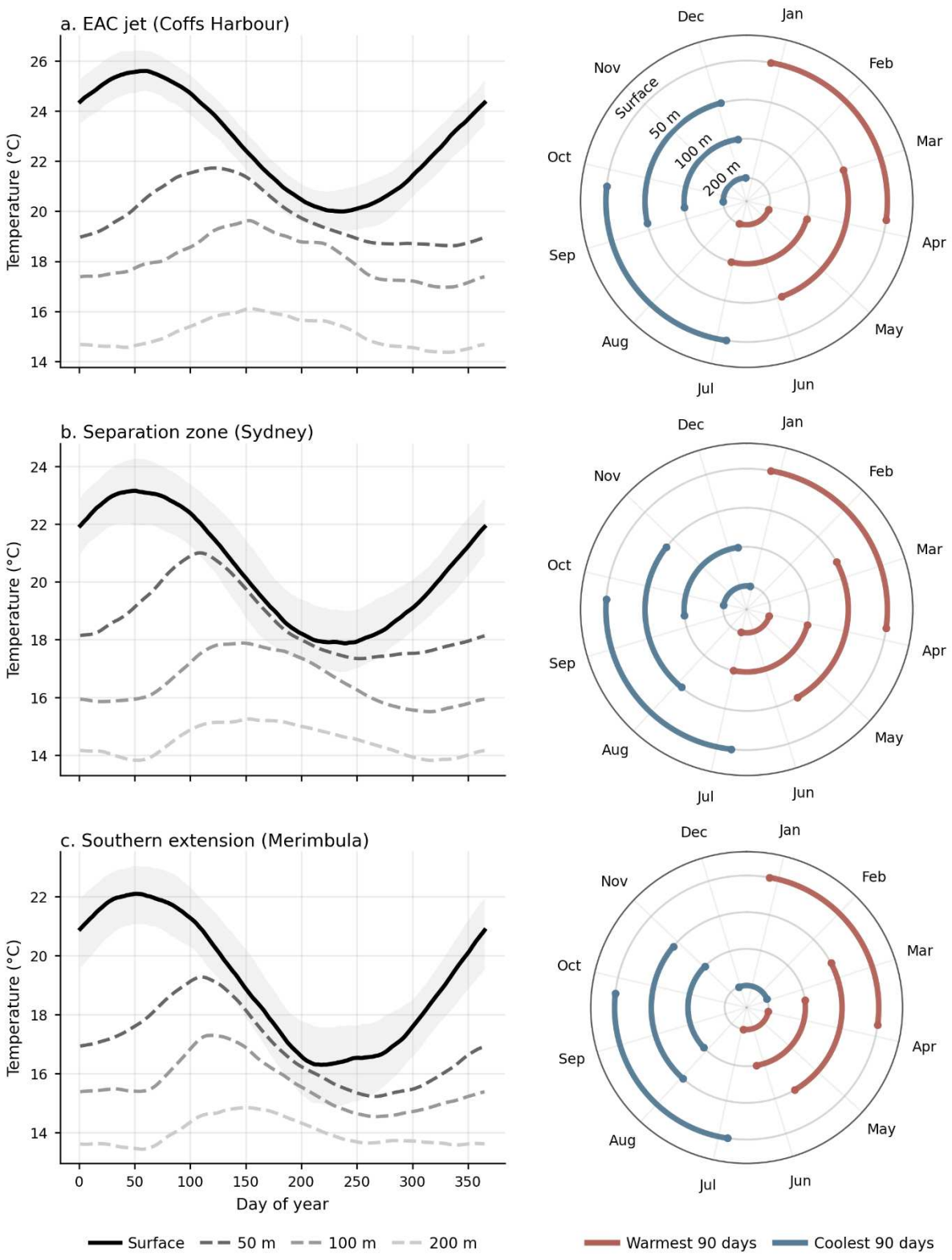


Figure 6: Temperature climatologies for surface and seafloor at specific seafloor depths of 50m 100m, and 200m across the three oceanographic regimes (by latitudinal bands). The black lines represent mean climatology with the grey shaded area the 10th and 90th percentile climatology for the surface. The right column represents the mismatch between the seasonal 90-day warmest period (red lines) and 90-day coolest period (blue lines) at different seafloor depths, where each ring represents a different isobathic depth with the outside ring representing surface metrics and seafloor depth decreasing to the inner most ring 200m.

The weighting was therefore designed to identify events occurring during climatologically warmer or cooler periods, while accounting for these spatial and depth-dependent differences. Seasonal weighting was applied to event duration and intensity and were quantified independently for each grid cell to accurately reflect the background seasonal structure. The strength of the seasonal cycle was quantified from the smoothed mean climatology as:

$$\mathrm{A} = \mathrm{Q}_{95}(\mathrm{T}_{50}) - \mathrm{Q}_{05}(\mathrm{T}_{50}) \tag{2}$$

Where Q_{95} and Q_{05} denote the 9^{5th} and 5th percentile of the T_{50} climatology. Therefore, A is the typical strength of the seasonal cycle. This was converted into a continuous index using linear scaling as follows:

$$\mathrm{S} = \frac{A}{A_{max}} \tag{3}$$

Where A_{max} is the maximum value of seasonal amplitude A across the region, and S as the resulting seasonal index. Therefore, areas with weak seasonal cycles exhibit low values of S and areas with high seasonal cycles exhibit high values of S. The relative thermal position of each day within the annual cycle was derived from the mean climatology and expressed as an index ranging from -1 to 1 as:

$$h(d) = 2\left(\frac{T_{50}(d) - T_{min}}{T_{max} - T_{min}}\right) - 1 \tag{4}$$

Where $T_{50}(d)$ is the daily mean climatology on a given day, and T_{min} and T_{max} are the minimum and maximum values of T_{50} for each pixel. Therefore $h(d)$ is the relative thermal placement for each day of year where $h(d) = -1$ corresponds to the coldest climatological conditions and $h(d) = 1$ is the warmest climatological condition with $h(d) = 0$ as the thermal midpoint of the annual cycle. The overall seasonal weighting is therefore expressed as follows:

$$W(d) = 1 + \alpha S\, h(d) \quad (5)$$

Where $h(d)$ describes the relative position of the day within the local climatological cycle. S quantifies the strength of the seasonality at each pixel. Seasonal weighting is therefore the greatest where a pronounced seasonal cycle exists and for events occurring towards the climatological thermal extremes. α was set to 0.1 to control the maximum degree of seasonal redistribution as it was the largest value that preserved the overall spatial rankings (see sensitivity analysis section). The strength of the seasonal weighting (α) was selected using a sensitivity analysis, with candidate values for α tested in increments of 0.05 through 0 to 1. For each value, spatial risk patterns were compared to the unweighted case ($\alpha = 0$) using rank correlation, hotspot overlap and the Jaccard index. The final value ($\alpha = 0.1$) was selected as the highest level of seasonal scaling that produced a detectable contribution to the framework while preserving the overall spatial structure of risk. Therefore, the formula redistributes risk toward the climatological thermal extremes, but only in regions and depths where a sufficiently strong seasonal cycle exists. The resulting seasonal weighting exhibits smooth behaviour across the regions and depths and was applied across individual MHW events. MHW metrics were then aggregated annually and summarised over the entire 26-year period to describe the weighted mean duration and mean intensity of MHWs.

In addition to seasonal variability, the framework incorporates long-term warming to account for spatial differences in background warming, allowing for locations with stronger background warming relative to the region to be considered higher risk. The long-term warming modulator was calculated as a per area linear SST trend over the 26-year period which was then normalised against the mean trend for the region scaled by 0.9 (see sensitivity analysis section) to ensure that the long-term warming contributes proportionally to the

overall risk index without dominating MHW components. Therefore, long term warming is represented as:

$$W = 1 + 0.9\left(\frac{(\Delta T/\Delta t)_{pixel}}{(\Delta T/\Delta t)_{mean}}\right) \quad (6)$$

Where W is the final warming term, $1 + 0.9$ represent the baseline risk and the weighting strength. $(\Delta T/\Delta t)_{pixel}$ is the per pixel linear SST change and $(\Delta T/\Delta t)_{mean}$ is the mean trend across the region. A separate sensitivity test confirmed this scaling was appropriate and did not disproportionately inflate risk in stronger warming regions.

Sensitivity analysis

Spearman rank correlation was used to quantify how the ordering of risk values changes with α where pixels are ranked from lowest to highest risk across weighted cases and the correlation between these ranks are computed. Values close to 1 indicate that seasonal weighting preserves the overall spatial ranking of risk, whereas lower values indicate increasing reordering of pixels. Hotspot overlap was then used to assess if the same spatial locations remain classified as high risk as α increases. Hotspots were defined as pixels within the upper 20% of risk values within each region, representing the areas of elevated risk. Although a 10% threshold is commonly used, here it identified too few pixels to characterise meaningful spatial patterns, hence a 20% threshold was applied. Hotspot overlap was calculated as the proportion of hotspot pixels where α=0 that were identified as hotspots after weighted seasonal α was calculated. Where high hotspot overlap values indicate that seasonal weighting preserves the identity and location of high-risk areas, whereas lower values indicate loss or replacement of hotspot pixels. Finally, the Jaccard index was used to quantify changes in the extent and composition of hotspot areas between the weighted and unweighted cases. For each value α the index calculates the number of pixels classified as high risk in

both the weighted and unweighted cases, divided by the total number of pixels classified as high risk in either case. This accounts for both the retention and gain or loss of hotspot pixels, where values closer to 1 indicate strong agreement in hotspot extent and composition while lower values indicate divergences between spatial hotspots. The largest value for which spatial ranking (Spearman ≥ 0.99) and the identity of high-risk pixels (≥90% overlap and Jaccard ≥0.82 of the top decile) were preserved across all regions was selected (figure S4; S5).

Data Availability

Model output is available at https://doi.org/10.5281/zenodo.12703063 and should be cited as Li et al. (2024). Shelf mooring data are available at the Australian Ocean Data Network (www.aodn.org.au) (IMOS, 2022). The Coral temp daily sea surface temperature data are available at NOAA Coral Reef Watch (**https://coralreefwatch.noaa.gov**)[59].

Code Availability

The spatial hazard index calculation and associated code is available here: https://github.com/stephwoolley/MHW_risk_framework

References

1. Hoey, A. S. *et al.* Recent Advances in Understanding the Effects of Climate Change on Coral Reefs. *Diversity* **8**, 12 (2016).
2. Smith, K. E. *et al.* Biological Impacts of Marine Heatwaves. *Annual Review of Marine Science* **15**, 119–145 (2023).
3. Capotondi, A. *et al.* A global overview of marine heatwaves in a changing climate. *Commun Earth Environ* **5**, 1–17 (2024).
4. Frölicher, T. L., Fischer, E. M. & Gruber, N. Marine heatwaves under global warming. *Nature* **560**, 360–364 (2018).

5. Smith, K. E. *et al.* Global impacts of marine heatwaves on coastal foundation species. *Nat Commun* **15**, 5052 (2024).
6. Smale, D. A. *et al.* Marine heatwaves threaten global biodiversity and the provision of ecosystem services. *Nat. Clim. Chang.* **9**, 306–312 (2019).
7. Filbee-Dexter, K. *et al.* Marine heatwaves and the collapse of marginal North Atlantic kelp forests. *Sci Rep* **10**, 13388 (2020).
8. Intergovernmental Panel On Climate Change (Ipcc). *The Ocean and Cryosphere in a Changing Climate: Special Report of the Intergovernmental Panel on Climate Change*. https://www.cambridge.org/core/product/identifier/9781009157964/type/book (2022) doi:10.1017/9781009157964.
9. Kajtar, J. B. *et al.* A stakeholder-guided marine heatwave hazard index for fisheries and aquaculture. *Climatic Change* **177**, 26 (2024).
10. Boyce, D. G. *et al.* A climate risk index for marine life. *Nat. Clim. Chang.* **12**, 854–862 (2022).
11. Higuera Roa, O. *et al.* Challenges and opportunities in climate risk assessment: future directions for assessing complex climate risks. *Environ. Res. Lett.* **20**, 053003 (2025).
12. Galli, G., Solidoro, C. & Lovato, T. Marine Heat Waves Hazard 3D Maps and the Risk for Low Motility Organisms in a Warming Mediterranean Sea. *Front. Mar. Sci.* **4**, (2017).
13. Schaeffer, A. & Roughan, M. Subsurface intensification of marine heatwaves off southeastern Australia: The role of stratification and local winds. *Geophysical Research Letters* **44**, 5025–5033 (2017).
14. Schaeffer, A., Sen Gupta, A. & Roughan, M. Seasonal stratification and complex local dynamics control the sub-surface structure of marine heatwaves in Eastern Australian coastal waters. *Commun Earth Environ* **4**, 1–12 (2023).

15. Hobday, A. J. *et al.* A hierarchical approach to defining marine heatwaves. *Progress in Oceanography* **141**, 227–238 (2016).
16. Jacox, M. G. *et al.* Global seasonal forecasts of marine heatwaves. *Nature* **604**, 486–490 (2022).
17. Hobday, A. J., Oliver, E. C. J., Gupta, A. S., Benthuysen, J. A. & Burrows, M. T. Categorizing and Naming Marine Heatwaves | Oceanography. https://tos.org/oceanography/article/categorizing-and-naming-marine-heatwaves (2018).
18. Marine heatwave forecast. *Moana Project* https://www.moanaproject.org/marine-heatwave-forecast.
19. Australian climate outlooks. https://www.bom.gov.au/climate/ocean/long-range-forecasts/?variable=ssta&region=AUS.
20. Hartog, J. R., Spillman, C. M., Smith, G. & Hobday, A. J. Forecasts of marine heatwaves for marine industries: Reducing risk, building resilience and enhancing management responses. *Deep Sea Research Part II: Topical Studies in Oceanography* **209**, 105276 (2023).
21. Konsta, K., Doxa, A., Katsanevakis, S. & Mazaris, A. D. Projected marine heatwaves over the Mediterranean Sea and the network of marine protected areas: a three-dimensional assessment. *Climatic Change* **178**, 17 (2025).
22. Holbrook, N. J. *et al.* Keeping pace with marine heatwaves. *Nat Rev Earth Environ* **1**, 482–493 (2020).
23. Großelindemann, H., Ryan, S., Ummenhofer, C. C., Martin, T. & Biastoch, A. Marine Heatwaves and Their Depth Structures on the Northeast U.S. Continental Shelf. *Front. Clim.* **4**, 857937 (2022).
24. Fragkopoulou, E. *et al.* Marine biodiversity exposed to prolonged and intense subsurface heatwaves. *Nat. Clim. Chang.* **13**, 1114–1121 (2023).

25. Sun, D., Li, F., Jing, Z., Hu, S. & Zhang, B. Frequent marine heatwaves hidden below the surface of the global ocean. *Nat. Geosci.* **16**, 1099–1104 (2023).
26. Oliver, E. C. J. *et al.* Marine Heatwaves. *Annual Review of Marine Science* **13**, 313–342 (2021).
27. Zhang, Y., Du, Y., Feng, M. & Hobday, A. J. Vertical structures of marine heatwaves. *Nat Commun* **14**, 6483 (2023).
28. Malan, N. *et al.* Lifting the lid on Marine Heatwaves. *Progress in Oceanography* **239**, 103539 (2025).
29. Pyle, R. L. & Copus, J. M. Mesophotic Coral Ecosystems: Introduction and Overview. in *Mesophotic Coral Ecosystems* (eds Loya, Y., Puglise, K. A. & Bridge, T. C. L.) 3–27 (Springer International Publishing, Cham, 2019). doi:10.1007/978-3-319-92735-0_1.
30. He, Q. *et al.* Common occurrences of subsurface heatwaves and cold spells in ocean eddies. *Nature* **634**, 1111–1117 (2024).
31. Bell, J. J. *et al.* Global status, impacts, and management of rocky temperate mesophotic ecosystems. *Conservation Biology* **38**, e13945 (2024).
32. Benedetti-Cecchi, L. *et al.* Marine protected areas promote stability of reef fish communities under climate warming. *Nat Commun* **15**, 1822 (2024).
33. Bruno, J. F. *et al.* Climate change threatens the world's marine protected areas. *Nature Clim Change* **8**, 499–503 (2018).
34. Soares, M. D. O. *et al.* Why do mesophotic coral ecosystems have to be protected? *Science of The Total Environment* **726**, 138456 (2020).
35. Wong, R. H. X., Monk, J., Perkins, N. R. & Barrett, N. S. A systematic review on the anthropogenic stressors on sessile benthic mesophotic reef communities: implications for temperate reef management in Australia. *Front. Mar. Sci.* **10**, (2023).

36. Rocha, L. A. *et al.* Mesophotic coral ecosystems are threatened and ecologically distinct from shallow water reefs. *Science* **361**, 281–284 (2018).
37. Biscaia Zamoner, J. *et al.* Integrating Oceanographic Data and Benthic Community Structure Temporal Series to Assess the Dynamics of a Marginal Reef. *Front. Mar. Sci.* **8**, (2021).
38. Amaya, D. J. *et al.* Bottom marine heatwaves along the continental shelves of North America. *Nat Commun* **14**, 1038 (2023).
39. Alexander, M. A., Scott, J. D., Jacox, M. G., Amaya, D. J. & Wilczynski, L. M. Processes That Influence Bottom Temperatures in the California Current System. *Journal of Geophysical Research: Oceans* **130**, e2024JC021886 (2025).
40. Elzahaby, Y. & Schaeffer, A. Observational Insight Into the Subsurface Anomalies of Marine Heatwaves. *Front. Mar. Sci.* **6**, (2019).
41. Cao, X., Li, C., Hu, Y., Yao, Y. & Li, J. Understanding bottom and surface marine heatwaves along the continental shelf of China. *Environ. Res. Lett.* **19**, 074062 (2024).
42. Holbrook, N. J. *et al.* A global assessment of marine heatwaves and their drivers. *Nat Commun* **10**, 2624 (2019).
43. Schlegel, R. W., Oliver, E. C. J. & Chen, K. Drivers of Marine Heatwaves in the Northwest Atlantic: The Role of Air–Sea Interaction During Onset and Decline. *Front. Mar. Sci.* **8**, (2021).
44. Fernandes, M., Vieira da Silva, C. & Frazão Santos, C. Climate-Related Vulnerability and Risk Assessment of Main Ocean Uses: An Overview. *Front. Mar. Sci.* **9**, (2022).
45. Jones, M. C. & Cheung, W. W. L. Using fuzzy logic to determine the vulnerability of marine species to climate change. *Global Change Biology* **24**, e719–e731 (2018).

46. Heidmann, S. L. *et al.* Depth and structure as environmental drivers of fish communities across a shallow to mesophotic gradient in the northern US Virgin Islands. *Bulletin of Marine Science* **100**, 133–154 (2024).
47. Lindfield, S. J., Harvey, E. S., Halford, A. R. & McIlwain, J. L. Mesophotic depths as refuge areas for fishery-targeted species on coral reefs. *Coral Reefs* **35**, 125–137 (2016).
48. Bell, J. J. *et al.* Marine heat waves drive bleaching and necrosis of temperate sponges. *Current Biology* **33**, 158-163.e2 (2023).
49. Wolfe, B. W. *et al.* Continental-Scale Assessment of Climate-Driven Marine Species Range Extensions Using a Decade of Citizen Science Data. *Diversity and Distributions* **31**, e70022 (2025).
50. Davies, T. E., Maxwell, S. M., Kaschner, K., Garilao, C. & Ban, N. C. Large marine protected areas represent biodiversity now and under climate change. *Sci Rep* **7**, 9569 (2017).
51. Champion, C. & Coleman, M. A. The emerging need for marine heatwave response plans: A globally relevant example from New South Wales, Australia. *Ocean & Coastal Management* **261**, 107526 (2025).
52. O'Regan, S. M., Archer, S. K., Friesen, S. K. & Hunter, K. L. A Global Assessment of Climate Change Adaptation in Marine Protected Area Management Plans. *Front. Mar. Sci.* **8**, (2021).
53. Cetina-Heredia, P., Roughan, M., van Sebille, E. & Coleman, M. A. Long-term trends in the East Australian Current separation latitude and eddy driven transport. *Journal of Geophysical Research: Oceans* **119**, 4351–4366 (2014).
54. Oke, P. R. *et al.* Revisiting the circulation of the East Australian Current: Its path, separation, and eddy field. *Progress in Oceanography* **176**, 102139 (2019).

55. Oke, P. R., Rykova, T., Sloyan, B. M. & Ridgway, K. R. What Causes the Subsurface Velocity Maximum of the East Australian Current? https://doi.org/10.1175/JPO-D-23-0128.1 (2024) doi:10.1175/JPO-D-23-0128.1.
56. Elzahaby, Y., Schaeffer, A., Roughan, M. & Delaux, S. Oceanic Circulation Drives the Deepest and Longest Marine Heatwaves in the East Australian Current System. *Geophysical Research Letters* **48**, e2021GL094785 (2021).
57. Wu, L. *et al.* Enhanced warming over the global subtropical western boundary currents. *Nature Clim Change* **2**, 161–166 (2012).
58. Li, J., Roughan, M. & Kerry, C. Variability and Drivers of Ocean Temperature Extremes in a Warming Western Boundary Current. *Journal of Climate* **35**, 1097–1111 (2022).
59. NOAA Coral Reef Watch. NOAA Coral Reef Watch Version 3.1 Daily 5km Satellite Regional Virtual Station Time Series Data for Southeast Florida, Mar. 12, 2013–Mar. 11, 2014. NOAA Coral Reef Watch (2019).
60. Mayorga Adame, C. G., Li, J., Kerry, C. & Roughan, M. Hydrodynamic daily climatology of South Eastern Australia based on a 22 year run of the SEA-COFS model. Zenodo https://doi.org/10.5281/zenodo.14063981 (2024).
61. McDougall, T. & Barker, P. M. Getting started with TEOS-10 and the Gibbs Seawater (GSW)Oceanographic Toolbox. *SCOR/IAPSO WG* **127**, 1–28 (2011).
62. IMOS, (2026), Australian national mooring network (ANMN) facility – Temperature and salinity time-series Retrieved from https:// thredds.aodn.org.au /thredds /catalog /IMOS/ANMN/NSW/catalog.html
63. Schlegel, R. W., Oliver, E. C. J., Hobday, A. J. & Smit, A. J. Detecting Marine Heatwaves With Sub-Optimal Data. *Front. Mar. Sci.* **6**, (2019).

Supplementary Files

This is a list of supplementary files associated with this preprint. Click to download.

- Supplementary.docx